Optik - International Journal for Light and Electron Optics 200 (2020) 163272

Contents lists available at ScienceDirect

Optik

journal homepage: www.elsevier.com/locate/ijleo

Original research article

Error compensation and accuracy analysis of laser measurement system based on laser-beam calibration

Jie Lu, Zhiqin Cai*, Bin Yao, Sijie Cai, Xiaofan Ma, Wanshan Liu

School of Aerospace Engineering, Xiamen University, Xiamen, China

ARTICLE INFO

Keywords:
Accuracy measurement
Error compensation
Laser displacement sensor
Laser calibration
Iterative function
Measurement strategy

ABSTRACT

In this paper, a novel measurement strategy, based on a 4D error-compensation model for the measurement of free-form surfaces in laser measurement systems, is presented. To improve the measurement accuracy, effects of the inclination angle and the azimuth angle (including the rotation angle and the deflection angle) on the measurement results are investigated experimentally. Considering the error compensation and the constructing iterative function, a calibration method for arbitrary positions and orientations of the laser-beam is presented, and a corresponding measurement strategy is presented. To verify the effectiveness and accuracy of the proposed measurement strategy, calibration schemes of a check bar geometry center are studied based on a 4-axis measuring platform. The obtained results demonstrate that the proposed strategy can greatly improve the measurement accuracy.

1. Introduction

As a mature non-contact measurement method, laser triangulation method has been widely used in the industrial production site owing to its high measurement precision, strong interference resistance, simple structure and flexible application [1]. By integrating laser triangulation method with the existing high precision measurement system, it is possible to realize the high-precision measurement of complex surface profile with a laser displacement sensor (the LDS). The error factors of laser triangulation method can be categorized into 4 classes:1) Imaging system error; 2) Data processing error and system installation error; 3) Errors caused by environmental factors such as temperature and humidity; 4) Errors caused by measured surface properties, which is mainly represented by the displacement deviation error caused by surface color, roughness, inclination angle and azimuth angle, et al. For existing laser displacement sensors, the data processing error, system installation error, lens distortion, and environmental factors have been effectively controlled. Therefore, the main factor influencing the accuracy of laser triangulation method is induced by the geometric properties of the measured surface [2–7].

To calibrate the position and direction of laser-beam, a new calibration method of laser-beam direction was presented to implement any-orientation measurement for point laser sensors in reverse engineering by Lu [8]. A calibration method suitable for a laser probe in on-machine laser scanning measurement was proposed to eliminate the measuring errors from installation pose by Zhang [9]. However, in all of the researches listed above, error-compensation, including the effects of inclination angle and azimuth angles (the rotation angle and the deflection angle) on the measurement accuracy, and so on, has not been considered. In the error-compensation model for the laser measurement, a novel measurement strategy and an error-compensation model for the measurement of large-scale free-form surfaces in on-machine laser measurement systems were presented by Li [10]. To improve the

* Corresponding author.
E-mail address: caizhiqin@xmu.edu.cn (Z. Cai).

https://doi.org/10.1016/j.ijleo.2019.163272
Received 24 August 2018; Received in revised form 16 July 2019; Accepted 20 August 2019

measurement accuracy, the effects of the scan depth, surface roughness and incident angle on the measurement results were investigated experimentally; A new error compensation strategy and the method of calculating incidence angle were proposed by Sun [11]. It can effectively improve the measurement accuracy of free-form surfaces by inclination error compensation; In considering of the measurement error of the laser displacement sensor due to the inclination of the measuring point, a quantifiable inclination error model was proposed by Li [12]. To establish the traceability of on-machine measurement with workpiece rotation, considering machine geometric errors and workpiece setup errors, the kinematic modeling and error sensitivity analysis for measured profiles were achieved by Ibaraki [13,14]. To correct the sensor's measurement errors caused by the inclination angle of measured point, an inclination error model was built to compensate data in real time, and a new wavelet threshold function was proposed to process data by Dong [15]. Based on the analysis of the cause of the color error and perform simulations, a color error compensation method, according to the error of the different colors, was proposed experimentally by Li [16]. Aiming at the measurement uncertainties caused by scattering surfaces and reflectivity variations cause, a new laser line triangulation measurements algorithm is proposed based on Chan–Vese model by Mueller [17]. However, to improve the measurement accuracy of the complex surface, it is not sufficient and reliable only to consider the scan depth, surface roughness, color, and inclination angle of the measured surface. The effect of other geometric properties of the measured surface cannot be ignored, such as color, roughness, the material of measured surface and azimuth angle (including rotation angle and deflection angle), et al.

The aims of this paper are: (1) to define the inclination angle and azimuth angles (such as rotation angle and deflection angle), then experimentally analyse the effects of these influence factors on laser measurement accuracy; (2) to build a 4D error-compensation model for the measurement of free-form surfaces in laser measurement systems; (3) to present an accurate measurement strategy suitable for any arbitrary position and direction of laser- beam based on the above considerations.

2. Principle and error analysis of laser measurement system

2.1. Laser triangulation method

The LDS is a precision optical instrument designed based on the principle of laser triangulation. According to the measurement principle of the LDS, the defocusing phenomenon will cause the dispersion of image points, thereby reducing the measurement accuracy of the system [9]. As shown in Fig. 1, the position of the laser point x on the measured surface can be calculated according to the position of the spotx'.

As shown in Fig. 1, the displacement of the measured surface along the normal direction can be expressed as

$$x = \frac{ax' \sin\theta_2}{b\sin\theta_1 \pm x'\sin(\theta_1 - \theta_2)} \tag{1}$$

where a represents the object distance of the receiving lens; b represents the image distance of the receiving lens. When the object surface moves below the reference plane, the positive sign is taken, otherwise, the minus sign is taken.

It can be seen from Eq. (1) that the deviation between the real value and the standard value of x', a, b, θ_1, θ_2 will affect the measurement accuracy of the system, and the measurement error can be simplified as [11]

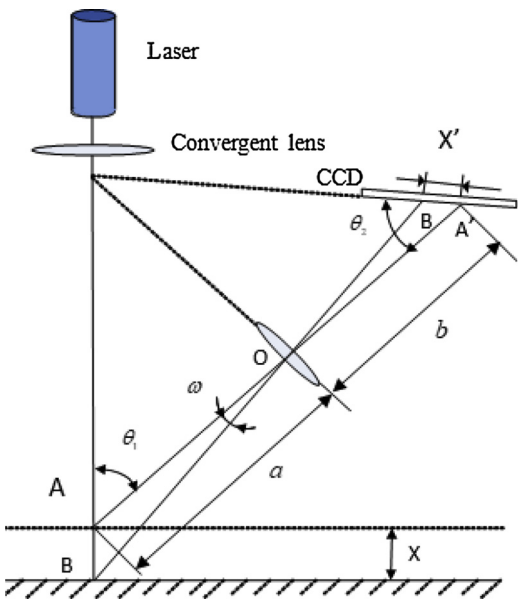

Fig. 1. Laser triangulation method.

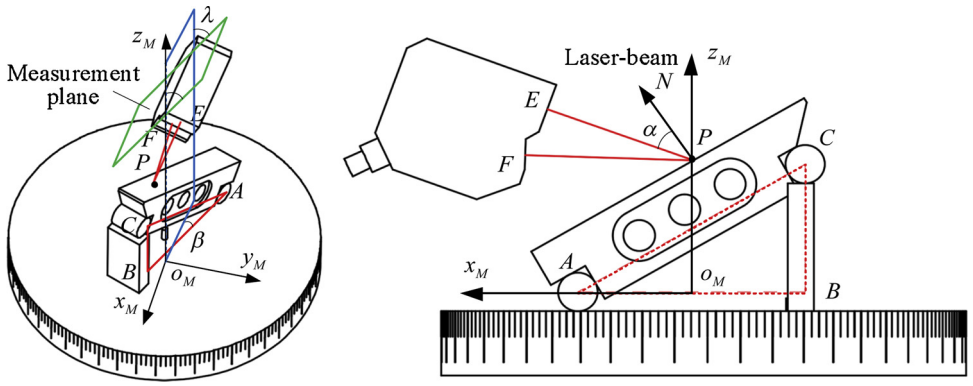

Fig. 2. Definition of calibration error term.

$$\delta x = \frac{\sin\left(arc\tan\left(\frac{\tan\theta_1}{\beta}\right)\right)}{\beta\sin\theta_1}\delta x' + \Delta\delta x \tag{2}$$

The deviation $\Delta\delta x$ is mainly influenced by the geometric properties of the measured surface, including error factors such as incident angle, incident angle and incident pendulum angle of the measured surface, as shown in Fig. 2.

2.2. Definition of the geometric properties

In this paper, a sine gauge is installed on the rotating turntable of the measuring platform. By composing the sine gauge and gauge blocks with different height, a certain surface inclination angle can be built, as shown in Fig. 2. The machine reference frame S_M (o_M-$x_My_Mz_M$) is established based on the rotary axis (C-axis), and the z_M-axis coincides with the C-axis. P represents the measured point of the surface, ***PN*** represents the normal direction of measured surface, ***EP*** represents the laser-beam, ***PF*** represents the receiving laser-beam, and $\triangle EPF$ represents the measuring plane of the LDS. ***AC*** and ***AB*** are parallel to the measured surface and the plane $\Delta x_M o_M y_M$, respectively, and the plane $\triangle ABC$ is vertical to the measured surface.

1) The angle between the laser-beam ***EP*** and the normal direction ***PN*** is defined as the inclination angle α. On the plane $\Delta x_M o_M z_M$, when the normal direction ***PN*** and the receiving laser-beam ***PF*** are defined at the different(same) side to laser-beam ***EP***, the inclination angle is positive(negative); 2) The angle between the measurement plane $\triangle EPF$ and the plane $\Delta x_M o_M z_M$ is defined as the deflection angle λ, it is positive(negative) when it is close to(away from) the positive direction of the y_M -axis; 3) On the plane $\Delta x_M o_M y_M$, the angle between the plane $\Delta x_M o_M z_M$ and the plane $\triangle ABC$ is defined as the rotation angle β, and it can be obtained by controlling the rotation angle of the turntable. The rotation angle is positive (negative) when measured surface revolving anti-clockwise (clockwise). When the measured plane $\triangle EPF$ is coplanar with the inclined plane $\triangle ABC$, the incident rotation angle is 0°.

Then the unit normal direction of the measured point-P in the coordinate system S_M can be expressed as

$$\boldsymbol{PN} = [n_x n_y n_z]^T \tag{3}$$

For the measured surface, ***PN*** is a known value. Assuming that the unit vector of laser-beam is ***EP***=$[l\ m\ n]^T$, then the inclination angle of point-P can be expressed as

$$\begin{aligned}\alpha &= \arccos\left(\frac{\boldsymbol{EP}\times\boldsymbol{PN}}{|\boldsymbol{EP}|\times|\boldsymbol{PN}|}\right)\\ &= \arccos(ln_x + mn_y + nn_z)\end{aligned} \tag{4}$$

Since the deflection angle error is not easy to be measured, it can be obtained by converting the deflection angle γ into the inclination angle α' and the rotation angle β'. The corresponding relationship is as shown in Fig. 3, the plane $\triangle LMN$ can be built through laser-beam ***EP*** and the normal direction ***PN***, and ***EP*** is parallel to ***LM***. The vertical line o_Mz_M of ***LM*** is established through measured point P, and o_M is the intersection. Reclosing and vertical to ***LM*** respectively, the coordinate system S_M (o_M-$x_My_Mx_M$) can be established. To accomplish the conversion, the measuring plane $\triangle E'PF'$ can be obtained by the plane $\triangle EPF$ rotates the deflection angle γ around the x_M-axis, and the converted plane $\triangle E'PF'$,$\triangle L'M'N'$ and the coordinate system $S_{M'}$ (o_M-$x_My_Mz_M$) can be obtained. Then the inclination angle α' can be confirmed by the normal direction ***PN*** of mea'sured surface and laser-beam ***EP'***, and the rotation angle β' can be defined as the angle between the plane $\triangle E'PF'$ and the plane $\triangle L'M'N'$.

Considering the effect of the deflection angle γ, the unit normal direction of point-P in the $S_{M'}$ coordinate system can be expressed as

$$\boldsymbol{PN} = \begin{bmatrix}\cos(\gamma) & \sin(\gamma) & 0\\ -\sin(\gamma) & \cos(\gamma) & 0\\ 0 & 0 & 1\end{bmatrix}\begin{bmatrix}n_x\\ n_y\\ n_z\end{bmatrix} = \begin{bmatrix}n_x\cos(\gamma) + n_y\sin(\gamma)\\ -n_x\sin(\gamma) + n_y\cos(\gamma)\\ n_z\end{bmatrix} \tag{5}$$

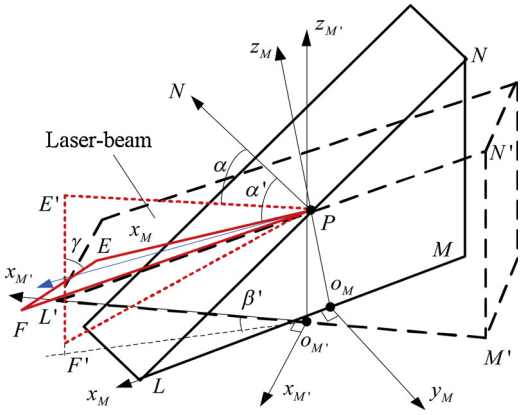

Fig. 3. Relationship between swing angle with incident angle and rotation angle.

Then the inclination angleα' is

$$\alpha' = \arccos\left(\frac{\boldsymbol{PN} \times \boldsymbol{E'P}}{|\boldsymbol{PN}| \times |\boldsymbol{E'P}|}\right) = \alpha \tag{6}$$

For convenience, suppose the z_M-axis coincides with the laser-beam $\boldsymbol{EP}$, and the x_M-axis coincides with $\boldsymbol{A'B'}$, then the normal vector of the plane $\triangle PNX_{M'}$ can be written as

$$\boldsymbol{n}=\begin{bmatrix} 0 \\ \frac{\cot\alpha}{\sin\gamma} \\ 1 \end{bmatrix} \tag{7}$$

For the LDS with arbitrary positions and orientations, the normal vector of the plane $\triangle PNX_{M'}$ can be represented as

$$\boldsymbol{n'} = \begin{bmatrix} 1 & 0 & 0 \\ 0 & \cos\theta_z & \sin\theta_z \\ 0 & -\sin\theta_z & \cos\theta_z \end{bmatrix} \begin{bmatrix} 0 \\ \frac{\cot\alpha}{\sin\gamma} \\ 1 \end{bmatrix} = \begin{bmatrix} 0 \\ \frac{\cot\alpha}{\sin\gamma}\cos\theta_z + \sin\theta_z \\ -\frac{\cot\alpha}{\sin\gamma}\sin\theta_z + \cos\theta_z \end{bmatrix} \tag{8}$$

where θ_z represents the angle between the laser-beam $\boldsymbol{EP}$ and the z_M-axis, which can be expressed as

$$\theta_z = \arccos\left(\frac{\boldsymbol{EP} \times \boldsymbol{OZ'}}{|\boldsymbol{EP}| \times |\boldsymbol{OZ'}|}\right) = \arccos(n) \tag{9}$$

Then, the relationship between the deflection angle γ with inclination angle α' and rotation angle β' can be expressed as

$$\begin{aligned} \beta' &= \arccos\left(\frac{\boldsymbol{n'} \times \boldsymbol{OY}}{|\boldsymbol{n'}| \times |\boldsymbol{OY}|}\right) \\ &= \arccos\left(\frac{\frac{\cot\alpha'}{\sin\gamma}\cos\theta_z + \sin\theta_z}{\sqrt{\left(\frac{\cot\alpha'}{\sin\gamma}\cos\theta_z + \sin\theta_z\right)^2 + \left(-\frac{\cot\alpha'}{\sin\gamma}\sin\theta_z + \cos\theta_z\right)^2}}\right) \end{aligned} \tag{10}$$

According to the Eq. (10), the error model of the deflection angle can be obtained by establishing the error model of the inclination angle and the rotation angle. Therefore, the LDS can be calibrated by three parameters, including the inclination angle, the rotation angle, and the scan depth.

2.3. Error proofreading experiment

The experimental device for error correction of laser measurement systems consists of an NC machining center, a LDS, a laser interferometer, a sine gauge, a standard gauge block, and an indexing plate. A Keyence LK-H050 laser displacement sensor is used as the demarcated displacement sensor, and the Renishaw XL-80 laser interferometer is used as the calibration benchmark, as shown in Fig. 4.

Before the experiment, the position and direction of the LDS should be precisely adjusted to ensure the vertical incidence of the laser-beam. Then the position of the interferometer component is adjusted to ensure that the optical path does not shift in the process of moving along the Z axis. Error correction experiment is set up with the inclination angle changes from $-45°$ to $45°$, the rotation angle changes from 0°to 10°, 90°, and 170°to 180°. The LDS moves along the Z-axis within the effective measurement range of the LDS (-10 mm to 10 mm), and the values of the LDS and the laser interferometer are recorded at per millimeter(1 mm).

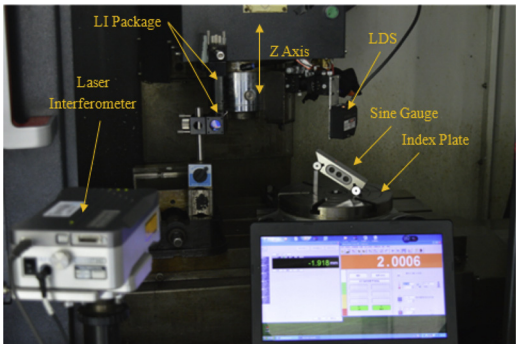

Fig. 4. Error proofreading experiment of the LDS.

More than 5000 groups of measured data of the LDS and laser interferometer are obtained. The difference between the LDS and laser interferometer is defined as the error of the LDS. The 4D error-compensation diagram of the LDS is established for inclination angle, rotation angle, scan depth, and measurement error, as shown in Fig. 5.

As shown in Fig. 6, according to the 4D error-compensation diagram, the inclination angles of 10°, 20°, 30°, 40°, and the rotation angles of 0°, 10°, 90°, 170°, 180° are selected for analysis, respectively. The results, fitting by the least square method, demonstrate that under different inclination angles or rotation angles, the effect of scan depth on measurement error can be modeled by lines with different slopes. The original error values can be obtained through the synthesis of straight lines and the angle transformation. The final compensation curve is shown as follows:

As shown in Fig. 6(a), when the laser scanning depth remains unchanged and with constant rotation angle, measurement error increases with the rising of inclination angle. The measurement error and inclination angle show nonlinear behavior, the deeper laser scan depth (the farther away from 0 mm), the more obvious the nonlinear performance, the poorer the error straightness and the greater the error variation. When the laser scanning depth is 0 mm, the error is 0 um, indicating that the measurement error of the LDS is not affected by the inclination angle; As shown in Fig. 6(b), when rotation angle remains unchanged and with the constant inclination angle, measurement error increases with its scanning depth. The correlation between measurement and scanning depth basically exhibits a linear relation. In the range of 0° to 180°, the absolute value of the measurement error increased after an initial decrease, and there are minimal measure errors when the rotation angle is about 90°. However, due to the existence of the inclination angle, there is still a certain linear error at 90°.

To summarize, in order to reduce the impact of inclination angle and azimuth angle to the laser measurement system, it is recommended to 1) keep a lower scan depth such that the linearity of the measurement error can be improved and the measurement precision after compensation can be ensured. 2) adjust the rotation angle such that it is stabilized at 90°, which lessens the impact of the rotation angle on measurement error. 3) pay more attention to the influence of the azimuth angle (including rotation angle and inflection angle). Although the influence of azimuth angle error on laser measurement accuracy is less comparing with inclination angle error.

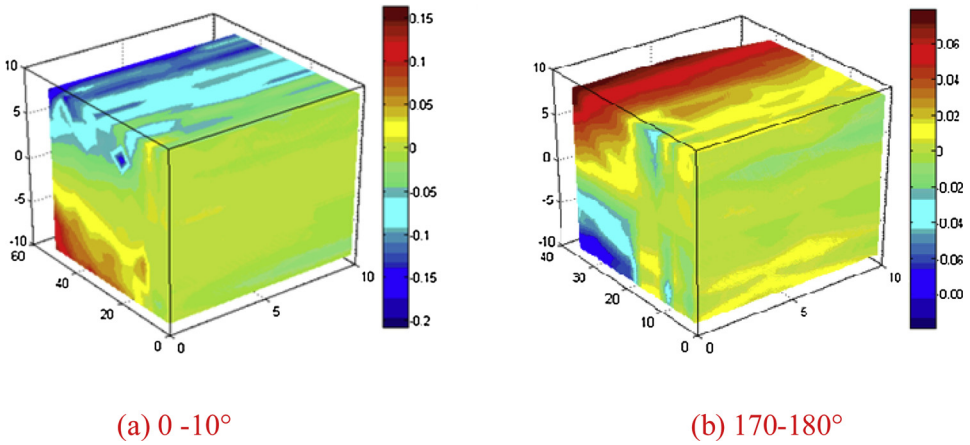

Fig. 5. 4D error-compensation diagram.

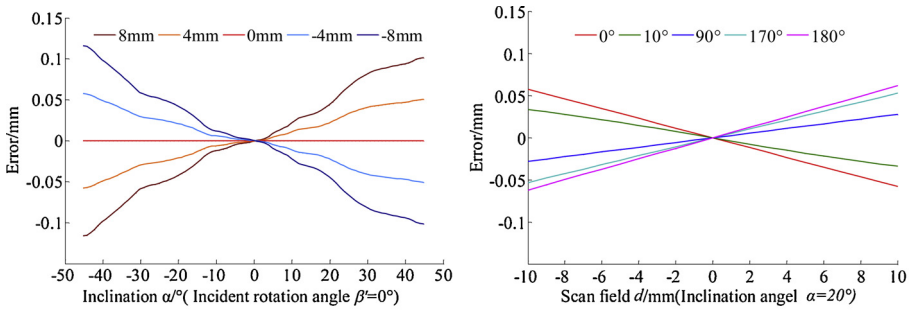

(a) the influence of α on measurement error (b) the influence of β on measurement error

Fig. 6. Error compensation curve.

3. Laser-beam calibration

3.1. The establishment and conversion of coordinate system

To improve the measurement accuracy of the LDS, the inclination angle must be controlled in a certain range, which requires the calibration of the position and direction of the LDS. For this, it is necessary to convert the measured value of the LDS from its coordinate system to the machine reference frame, which requires the establishment of three coordinate systems, as shown in Fig. 7.

(1) The coordinate system of the machine tool *O-XYZ*. The zero position of the *Y*-axis grating ruler is defined as the original point. The directions of the 3 axes are consistent with the 3 guide rails of the measuring machine, respectively.
(2) The coordinate system S_s (o_s-$x_s y_s z_s$) of the LDS. The zero position of the LDS is defined as the original point. The directions of the 3 axes are consistent with the *X/Y/Z* axis of the machine tool, respectively.
(3) Machine reference frame S_M (o_M-$x_M y_M z_M$). When the measuring machine is in the zero state and the scan depth of the LDS is 0 mm, this position is defined as the origin point. The directions of the 3 axes are consistent with the *X/Y/Z* axis of the machine tool respectively.

As shown in Fig. 7, the coordinate value of measured point in machine reference frame S_M can be directly obtained through the coordinate transformation from S_s to S_M.

$$\begin{bmatrix} x_M \\ y_M \\ z_M \\ 1 \end{bmatrix} = \begin{bmatrix} R_1 & T_1 \\ 0 & 1 \end{bmatrix} \cdot \begin{bmatrix} x_S \\ y_S \\ z_S \\ 1 \end{bmatrix} \tag{11}$$

Where $[x_S y_S z_S]^T$ is the measured value of the LDS in the S_s coordinate system. The unit vector of the laser-beam in S_s coordinate system are *l*, *m*, *n*, and the corresponding length is *d* (readout directly from the LDS), then $[x_S y_S z_S]^T = [ldmdnd]^T$. R_1 and T_1 represent the rotation matrix and translation matrix of S_s relative to S_M, respectively.

Since the axes of the above coordinate systems are parallel and uniform in direction, then

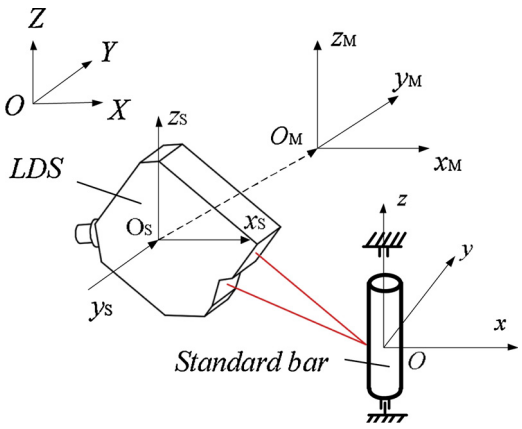

Fig. 7. Coordinate transformation process.

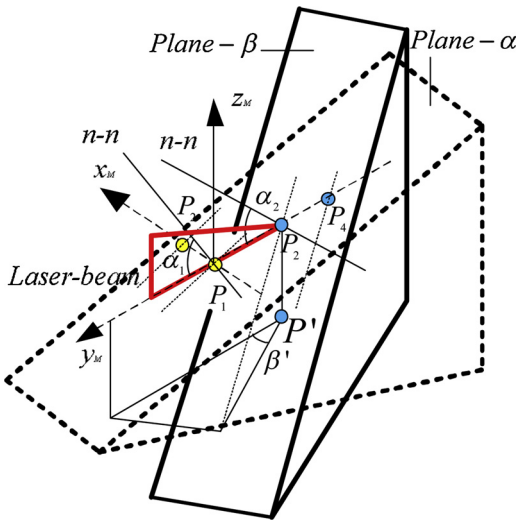

Fig. 8. Calibration process diagram of *l*, *m*, *n*.

$$\begin{bmatrix} x_M \\ y_M \\ z_M \\ 1 \end{bmatrix} = \begin{bmatrix} 1 & 0 & 0 & x_{M0} \\ 0 & 1 & 0 & y_{M0} \\ 0 & 0 & 1 & z_{M0} \\ 0 & 0 & 0 & 1 \end{bmatrix} \cdot \begin{bmatrix} ld \\ md \\ nd \\ 1 \end{bmatrix} = \begin{bmatrix} x_{M0} + ld \\ y_{M0} + md \\ z_{M0} + nd \\ 1 \end{bmatrix} \tag{12}$$

Through Eq. (12), the measured value in machine reference frame S_M can be obtained.

3.2. Design of calibration scheme

As shown in Fig. 8, the plane equation of the calibration plane $\alpha$is

$$Ax + By + Cz + D = 0 \tag{13}$$

where A, B, C are the normal vector of the planeα.

Assuming that P_1 represents the intersection point between the laser-beam and the plane α, the measurement value of the LDS is d_1, and the grating readings are x_{M1}, $y_{M1,}$ and z_{M1}, then

$$A(x_{M1} + ld_1) + B(y_{M1} + md_1) + C(z_{M1} + nd_1) + D = 0 \tag{14}$$

When the LDS moves Δx along the X-axis (Δx is the grating variation), the intersection point between the LDS and the plane α becomes P_2, the measurement value of the LDS turned into d_2, and the corresponding grating readings are $x_{M1} - \Delta x$, y_{M1} and z_{M1}, then

$$A(x_{M1} + ld_2 - \Delta x) + B(y_{M1} + md_2) + C(z_{M1} + nd_2) + D = 0 \tag{15}$$

Subtract Eq. (14) from Eq. (15), then Eq.(16) can be obtained after rearranging.

$$\begin{cases} A(l\Delta d_x + \Delta x) + B(m\Delta d_x) + C(n\Delta d_x) = 0 \\ \Delta d_x = d_1 - d_2 \end{cases} \tag{16}$$

Similarly, the LDS moves Δy along the Y-axis and moves Δz along the Z-axis, respectively, Eq. (17) can be obtained.

$$\begin{cases} A = U\Delta d_x/\Delta x \\ B = U\Delta d_y/\Delta y \\ C = U\Delta d_z/\Delta z \end{cases} \tag{17}$$

where the value $U = Al + Bm + Cn$ is a constant, and Eq. (18) can be obtained after simplification.

$$l\Delta d_x/\Delta x + m\Delta d_y/\Delta y + n\Delta d_z/\Delta z = 0 \tag{18}$$

Suppose $a_1 = \Delta d_x/\Delta x$, $b_1 = \Delta d_y/\Delta y$, $c_1 = \Delta d_z/\Delta z$, then

$$a_1 l + b_1 m + c_1 n = 0 \tag{19}$$

Similarly, when the LDS is intersected with the plane β, Eq. (20) can be obtained.

$$a_2 l + b_2 m + c_2 n = 0 \tag{20}$$

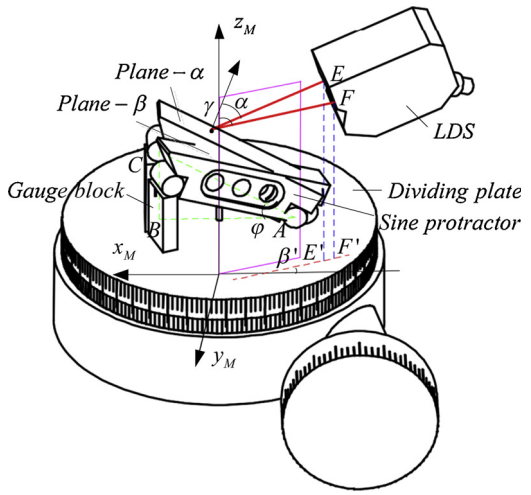

Fig. 9. Installation schematic diagram of calibration block.

Since

$$l^2 + m^2 + n^2 = 1 \tag{21}$$

Through Eqs. (19)–(21), the unit vector of laser-beam *l*,*m*,*n* can be obtained.

3.3. Design of calibration block

According to the sine gauge installed on the rotating turntable of the measuring platform, by adjusting the inclination angle and rotation angle of the sine gauge on the turntable, the plane α and the plane$\beta$are established, as shown in Fig. 9.

The plane α is determined by installing the sine gauge on the radial bisection line of the turntable, as shown in Fig. 9. In the S_M coordinate system, *AB* is the sine gauge length, and *BC* represents the height of the standard gauge block, the inclination angle of the sine gauge can be obtained by adjusting the height of the standard gauge block.

$$BC = AC \bullet \sin \varphi \tag{22}$$

When the basic parameters of the plane α is determined, the value of a_1,b_1,c_1 can be obtained on the basis of the proposed calibration scheme. Similarly, since the plane β depends on the relative position of the plane α and the height of sine gauge, the value of a_2, b_2, c_2 can also be obtained.

However, in practical measurement strategy, the measurement error exists in the measurement of the plane α and the plane β due to the effect of inclination angle and azimuth angle, which will lead to the error in the calibration of the unit direction vector *l*, *m* and *n* of laser-beam, and affects the measurement precision of the LDS. To improve the measurement accuracy, a compensation strategy is proposed as following:

(1) In the preliminary estimation of the position and direction of the laser beam, the initial inclination angle, rotation angle and deflection angle are obtained from the installation position of the LDS and the basic parameters of the plane α. The initial compensated values of a_1, b_1 and c_1 can be obtained by the error compensation curve.

$$\begin{cases} a_1 = (\Delta d_x + \varepsilon_x)/\Delta x \\ b_1 = (\Delta d_y + \varepsilon_y)/\Delta y \\ c_1 = (\Delta d_z + \varepsilon_z)/\Delta z \end{cases} \tag{23}$$

where, ε_x, ε_y, ε_z are the corresponding compensation.

It must be noted that, due to the influence of the scan depth and rotation angle, although the inclination angle remains unchanged for the same calibrated plane, when the LDS moves along the *X*/*Y*/*Z* axis, the relative scan depth and rotation angle between the measuring surface of the LDS and the measured surface are different.

(2) Similarly, the initial compensated values of a_2, b_2, and c_2 of the plane β can also be obtained by the error compensation curve, and the initial value of *l*,*m*,*n* can be acquired.

(3) Combined with the initial values of *l*,*m*,*n* and the basic parameters of the plane α and the plane β, the corresponding inclination angle, rotation angles, and deflection angle can be corrected, and the corrected values of *l*,*m*,*n* can be obtained.

Suppose the error function is $f(l, m, n, a_{1,2}, b_{1,2}, c_{1,2})$, the number of iterations is p, then the iterative formula can be expressed as:

If $p = 1$, the initial condition is

$$\begin{cases} \dfrac{\Delta d_{x_1}}{\Delta x_1} l_1 + \dfrac{\Delta d_{y_1}}{\Delta y_1} a_1 + \dfrac{\Delta d_{z_1}}{\Delta z_1} n_1 = 0 \\ \dfrac{\Delta d_{x_2}}{\Delta x_2} l_1 + \dfrac{\Delta d_{y_2}}{\Delta y_2} m_1 + \dfrac{\Delta d_{z_2}}{\Delta z_2} n_1 = 0 \\ l_1^2 + m_1^2 + n_1^2 = 1 \end{cases} \tag{24}$$

If $P > 1$

$$\begin{cases} \dfrac{\Delta d_{x_1} + l_{p-1} M}{\Delta x_1} l_p + \dfrac{\Delta d_{y_1} + m_{p-1} M}{\Delta y_1} m_p + \dfrac{\Delta d_{z_1} + n_{p-1} M}{\Delta z_1} n_p = 0 \\ \dfrac{\Delta d_{x_2} + l_{p-1} N}{\Delta x_2} l_p + \dfrac{\Delta d_{y_2} + m_{p-1} N}{\Delta y_2} m_p + \dfrac{\Delta d_{z_2} + n_{p-1} N}{\Delta z_2} n_p = 0 \\ l_p^2 + m_p^2 + n_p^2 = 1 \\ M = f(l_{p-1}, m_{p-1}, n_{p-1}, a_1, b_1, c_1) \\ N = f(l_{p-1}, m_{p-1}, n_{p-1}, a_2, b_2, c_2) \end{cases} \tag{25}$$

and the iterative conditions can be defined as

$$\begin{cases} f(l_p, m_p, n_p, a_1, b_1, c_1) - f(l_{p-1}, m_{p-1}, n_{p-1}, a_1, b_1, c_1) \le \varsigma \\ f(l_p, m_p, n_p, a_2, b_2, c_2) - f(l_{p-1}, m_{p-1}, n_{p-1}, a_2, b_2, c_2) \le \varsigma \end{cases} \tag{26}$$

After repeated iterations, until the values of l, m, n are stabilized within a certain precision range, the exact values of l, m, n can be obtained.

$$l = l_p,\ m = m_p,\ n = n_p \tag{27}$$

3.4. Calibration experiment for laser-beam

The LDS with arbitrary position and orientation is calibrated by the proposed method in this paper. In order to verify the accuracy of the theory, the proposed method is applied and compared with the known position and direction of laser-beam. The calibration schemes are researched based on the 4-axis measuring platform and using sine gauge calibration blocks, as shown in Fig. 10.

The calibration process of the laser beam is as follows:

(1) Combined with the height of calibration block and related installation parameters of sine gauge, the inclination angle, rotation angle, and deflection angle are determined by the basic parameters A, B, C of the plane α / β and the estimated installation posture of the LDS.
(2) Driving 4-axis measuring platform to adjust the distance between the LDS and the calibration plane α, so that the plane α can be measured in the measurable ranges of the LDS. Record the laser length d_1 and the initial coordinates of the measured point (x_1, y_1, z_1).
(3) Driving the LDS to move along the X-axis isometric. The measurement system sampling once at each step Δx, the laser length d_i and grating reading x_i on the X-axis are recorded respectively. Assuming that the feed number is n, then $n+1$ sets of compensated data $\{(d_i, x_i)\}_{i=1}^{n+1}$can be obtained, as shown in Table 1.
(4) The initial compensated values of a_1 can be obtained by Eq. (23), where

$$a_1 = \frac{\left(\sum_{i=1}^{n+1} \frac{(\Delta d_{xi+1} + \varepsilon_{xi+1}) - (\Delta d_{xi} + \varepsilon_{xi})}{\Delta x_{i+1} - \Delta x_i} \right)}{n} \tag{28}$$

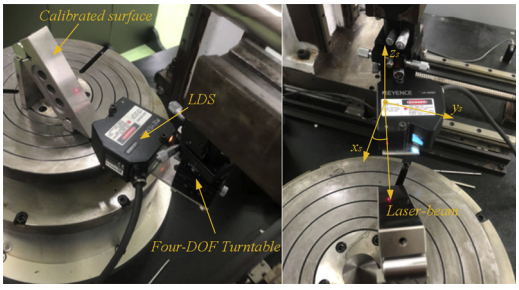

Fig. 10. Calibration experiment of the laser beam.

Table 1
Data of position and direction of laser-beam.

β	l	m	n	l'	m'	n'	α	α'	$\delta(20°)$
0°/20°	0.3362	0.005	0.9417	0.3442	0.002	0.9392	19.6507°	20.0823°	0.0823°
20°/40°	0.3384	0.006	0.9409	0.3409	0.003	0.9401	19.7865°	19.9316°	0.0684°
40°/60°	0.3473	0.004	0.9377	0.3428	0.001	0.9394	20.3295°	20.0489°	0.0489°
60°/80°	0.3366	0.002	0.9416	0.3436	0.001	0.9391	19.6737°	20.0990°	0.0990°
80°/90°	0.3389	0	0.9408	0.3417	0	0.9398	19.8136°	19.9820°	0.0180°
0°/90°	0.3473	0.003	0.9377	0.3406	0.002	0.9402	20.3278°	19.9148°	0.0852°

(5) Similarly, when the LDS moves Δy along the Y-axis or moves Δz along the Z-axis, the initial compensated value of b_1 or c_1 can be obtained
(6) Repeat the prior steps to obtain the initial compensated values of a_2, b_2, and c_2 of another calibrated plane β. Through Eq. (19)–(21), the initial unit vector of laser-beam l,m,n can be obtained.
(7) Suppose the error function is $f(l, m, n, a_{1,2}, b_{1,2}, c_{1,2})$, then after repeated iterations, the accurate value of l, m, n can be achieved, and the measurement strategy can be verified by comparing with the known value (accurately obtained through a four-DOF turntable, as shown in Fig. 10).

Suppose the average error $\overline{\delta}$ and standard deviation σ of the laser measurement system are

$$\begin{cases} \overline{\delta} = \dfrac{\sum_{i=1}^{n} \delta_i}{n} = 0.0670° \\ \sigma = \sqrt{\dfrac{\sum_{i=1}^{n} (\delta_i - \overline{\delta})^2}{n\text{-}1}} = 0.0268° \end{cases}$$

Then, in the range of 3σ, any measurement error may occur in the interval ($\overline{\delta}$ -3 σ, $\overline{\delta}$ +3 σ). That is, the measurement error of the LDS in any position and direction is $E = 0.0670° \pm 3 \times 0.0268°$. The experimental results show that, in the case of no compensation, the calibration error of the position and direction of the laser beam is larger, it can be effectively calibrated by the method described in this paper, and the calibrated LDS basically keeps the original measurement accuracy.

In practice, according to the results of the 4D error-compensation model, the inclination angle has a great influence on the measurement accuracy. Hence, to improve the compensation effect of inclination angle error, the smaller the inclination angle, the lower the scan depth, or the closer the rotation angle is to 90°, the higher the compensation accuracy.

4. Experimental verification

4.1. Measuring platform

The HJY054 Coordinate Measuring Machine (HJY054-CMM), produced by Hanjiang Machine Tool Co., Ltd, is adopted in this

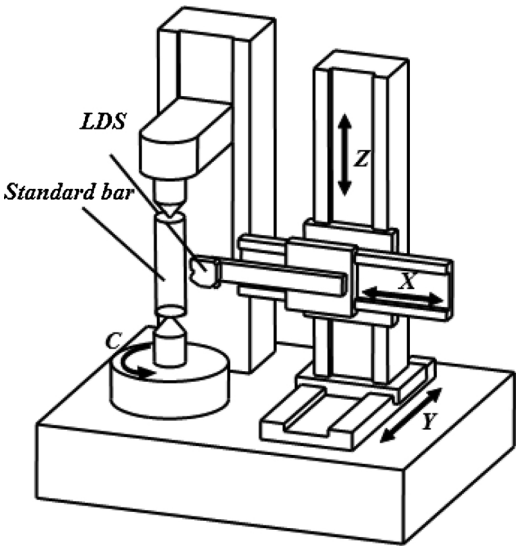

Fig. 11. Schematic diagram of measuring platform.

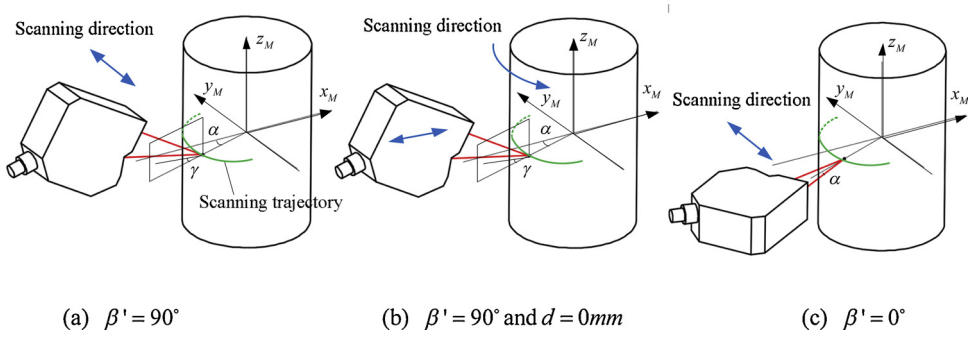

Fig. 12. Calibration experiment.

research, as shown in Fig. 11. The measuring instrument can realize movement along the three straight axes (*X/Y/Z*) as well as realizing workpiece rotation along the rotary axis (*C*). The LDS is installed at the *X*-axis and moves with the three straight axis (*X/Y/Z*), and the workpiece rotates about the C-axis. The Renishaw grating is used for position signal feedback in each axis. The LK-H050 laser displacement sensor is used as the laser probe (linearity: ± 4um, repeatability precision: 0.025um).

4.2. Calibration experiment for a check bar

This paper takes the calibration of a check bar (Diameter:50 mm, Precision: ± 2um) as an example to verify the accuracy of the theory. In the case of determining the position and direction of laser-beam, the measurement strategy is verified by the calibration experiment of the check bar. The concrete experimental scheme is as follows:

Scheme-1: The scan depth of the LDS is stable at 0 mm, as shown in Fig. 12(b), the grating value of the coordinate measuring instrument is directly read as the measured value, and the check bar center coordinates can be obtained through the corresponding coordinate transformation. In addition, some results can also be verified by this experiment as follows: 1) When the LDS is equivalent to a contact probe, whether the results could meet the requirement of precision detection; 2) When the LDS is used for precise measurement, whether the inclination angle, rotation angle, and deflection angle have an impact on the measurement accuracy.

Scheme-2: When the position and direction of laser-beam are determined, the measuring plane of the LDS is vertical or parallel to the axial direction of the standard rob respectively (that is, the installation rotation angles are 0° and 90° respectively), as shown in Fig. 12(c) and (a), the LDS scans horizontally within the measurement range, the measured values are obtained by the readings of the LDS and grating, and after obtaining the compensation from the above 4D error-compensation model, the check bar center coordinates can be obtained.

The compensated center coordinates of Scheme-2 are compared with the results obtained from Scheme-1, and the feasibility and accuracy of the measurement strategy are verified.

As shown in Fig. 13, the check bar is installed on the rotation axis of the measurement center through the upper and lower tip, and the axis of the check bar coincides with the *C*-axis. The laser probe is installed on the *X*-axis of the measurement center, and the measuring plane of the LDS is vertical or parallel to the axial direction of the standard rob respectively. The laser-beam travels along the *X*-axis and moves laterally along the *Y*-axis, and the laser-beam direction is known.

According to the above measurement schemes, controlling the servo system collects 20 sets of data points along with the *Y*-axis interval 2 mm, as shown in Table 2. The laser measurement values of Scheme -1 and Scheme-2 is compensated by the 4D error model

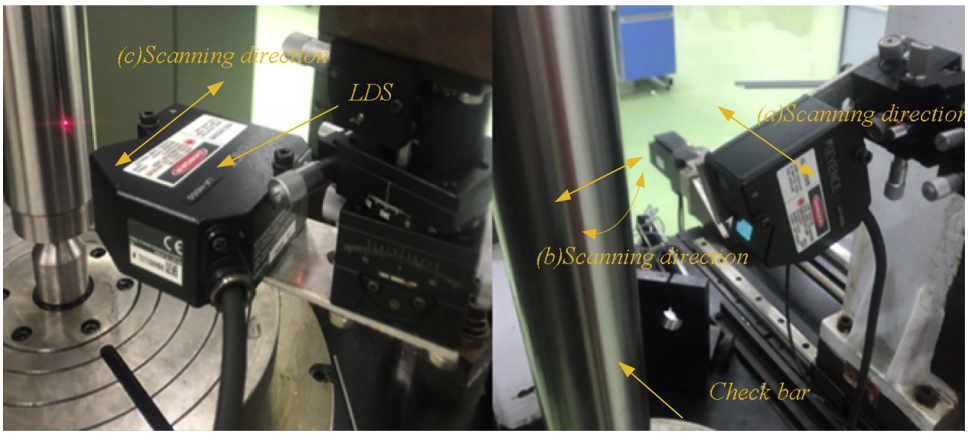

Fig. 13. Calibration experiment of a check bar.

Table 2
Data compensation results of the measurement schemes.

Scheme-2(0°)			Scheme-2(90°)			Scheme-1(0 mm)		Scheme-3	
Laser value	Compensation	Y-axis Grating value	Laser value	Compensation	Y-axis grating value	X-axis Grating value	Y-axis grating value	X-axis Grating value	Y-axis grating value
−4.273	−4.338	81.414	−2.345	−2.322	−90.242	159.892	−90.0757	3.537	7.167
−1.878	−1.901	79.413	−0.356	−0.354	−92.239	157.834	−92.1039	1.539	6.920
0.007	0.007	77.414	1.253	1.246	−94.244	156.213	−94.1168	−0.432	6.513
1.527	1.544	75.413	2.537	2.527	−96.234	154.881	−96.1332	−2.365	5.949
2.772	2.797	73.413	3.590	3.579	−98.237	153.850	−98.0827	−4.246	5.231
3.776	3.802	71.411	4.427	4.415	−100.235	153.023	−100.019	−6.063	4.364
4.561	4.590	69.419	5.064	5.055	−102.230	152.366	−102.026	−7.805	3.354
5.177	5.199	67.418	5.517	5.510	−104.233	151.895	−104.003	−9.459	2.207
5.58	5.465	65.418	5.830	5.807	−106.234	151.576	−105.988	−11.016	0.930
5.833	5.839	63.411	5.947	5.949	−108.230	151.490	−107.039	−12.465	−0.468
5.944	5.946	61.412	5.929	5.924	−110.236	151.420	−109.01	−9.375	−37.768
5.887	5.884	59.415	5.716	5.706	−112.238	151.514	−111.085	−7.715	−38.909
5.651	5.640	57.412	5.364	5.352	−114.243	151.788	−113.099	−5.969	−39.912
5.26	5.244	55.416	4.837	4.818	−116.229	152.215	−115.098	−4.149	−40.771
4.687	4.667	53.415	4.134	4.113	−118.229	152.800	−117.029	−2.265	−41.481
3.931	3.914	51.414	3.212	3.190	−120.238	153.598	−119.048	−0.330	−42.037
2.969	2.949	49.417	2.065	2.049	−122.239	154.592	−121.023	1.644	−42.436
1.784	1.769	47.417	0.665	0.658	−124.235	155.847	−123.042	3.643	−42.674
0.294	0.291	45.413	−1.070	−1.133	−126.236	157.408	−125.064	5.655	−42.751
−1.536	−1.513	43.417	−3.242	−3.283	−128.230	159.315	−127.065	7.667	−42.666

of the LDS (shown in Fig. 11).

Based on the least-square method, the center coordinates and radius of the check bar for the two schemes are fitted. The center coordinates and radius by Scheme-1 are (176.4216, −108.8332), 25.0026 mm.When the rotation angle is 0°, the measured center coordinates of the Scheme-2 are (−19.0844,61.236), and the radius is 25.0248 mm. The compensation is (−19.0462, 61.2481) and 24.9921 mm. The compared results shown that the measurement accuracy is improved by 16.9um. When rotation angle is 90°, the measured center coordinates of the Scheme-2 are (−19.0574, −108.8498), and 25.0128 mm, while the compensations are (−19.0576, −108.8324) and 25.0019 mm. The compared results shown that the measurement accuracy is improved by 10.9um.

These results show that: 1) The measurement error of Scheme-1 is 2.6um, and the measurement accuracy of Scheme-1 is highest. 2)Since the laser-beam of Scheme-1 is stable at 0 mm and the value directly read from the grating, the laser probe can be equivalent to the contact probe. The experimental results show that the error is very small and can meet the requirements of precision detection.

The comparison between Scheme-2 and Scheme-1 shows that if there is no compensation in Scheme-2, there is a large error in these two measurement results, which indicates that the laser measurement system is greatly influenced by external factors. After the error model compensation, the precision of the collected data is improved, the maximum error is 7.9 μm and the minimum error is 1.9 μm, and the fitting radius of the check bar is closer to the true value. This shows that Scheme-2 is the most suitable scheme when it is impossible to ensure that the laser probe is always in the position of 0 mm.

According to the maximum allowable value of surface roughness and geometric tolerance for a check bar, from the standard GB/T 17,421.1 (as shown in Table 3), the roundness of the check bar is 0.5um. Considering the influence of the machine motion error, the measurement accuracy meets the detection requirements.

To further verify the accuracy of the proposed method, in the same detection environment, the contact probe is used to verify the accuracy. The contact measuring platform is shown in Fig. 14.

The center coordinates and radius are (5.6021, −17.7491), 25.0018 mm, the maximum error is 1.8 um. Compared with the measured results by Scheme-1 (2.6um) and Scheme-2 (1.9um), the accuracy of the three methods is similar, which shows that the accuracy of the proposed methods is accepted.

5. Conclusion

In this paper, considering the effect of the inclination angle and azimuth angles, the corresponding error compensation curves are investigated experimentally, and a 4D compensation model for improving the measurement accuracy is put forward. To achieve

Table 3
Standard for cylindrical check bars.

No.	Items	Effective measurement length /mm	Tolerance/um	
			M-rated	P-rated
1	Roundness	≥315 ~ 500	0.25	0.5

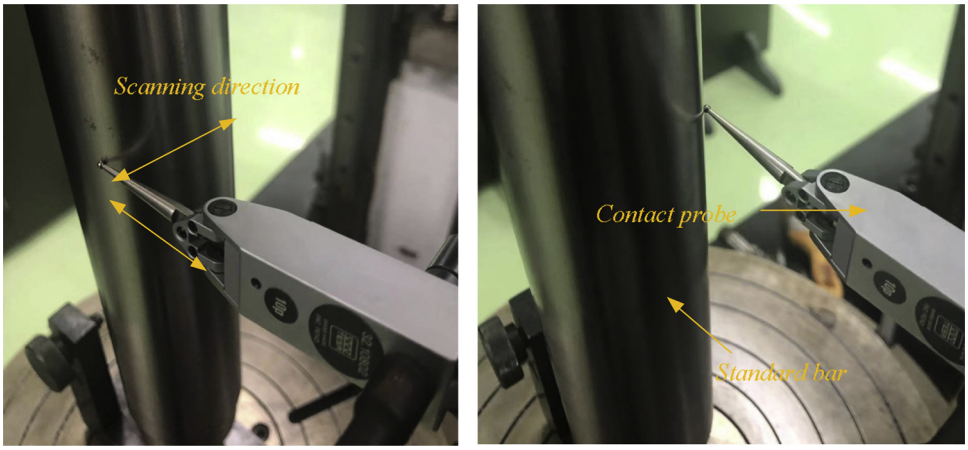

Fig. 14. Calibration experiment of the check bar followed by Scheme-3.

effective compensations, the mathematical model of inclination angle, incident rotation angle and incident swing angle of the measured surface at arbitrary position and direction of laser-beam are deduced, which can meet the error compensation of any measured point on the surface. On the basis of sine gauge calibration block with adjustable demarcation direction, the accurate position and orientation of the laser sensor is acquired by considering error compensation and constructing iterative function (including setting initial conditions, convergence conditions, and error functions). Ultimately, a practical measurement strategy suitable for any arbitrary position and direction of laser-beam is proposed.

Based on the compensation model, the effectiveness and accuracy of the measurement strategy are verified through the measurement of the geometry center of a check bar on a 4-axis measuring platform. The results demonstrate that the measurement strategy and the error compensation model can increase the measurement accuracy effectively.

Acknowledgments

This work was funded by Project of China Postdoctoral Science Foundation (No:2019M652256) and Intelligent Manufacturing Integrated Standardization and New Model Application Projects of the MIIT (No. 265 [2018]).

References

[1] E. Shafir, G. Berkovic, Optical methods for distance and displacement measurements, Adv. Opt. Photonics 4 (2012) 441–471.
[2] T. Mueller, A. Poesch, E. Reithmeier, Measurement uncertainty of microscopic laser triangulation on technical surfaces, Microsc. Microanal. 21 (2015) 1443–1454.
[3] X.Q. Li, Z. Wang, L.H. Fu, A laser-based measuring system for online quality control of car engine block, Sensors 16 (2016) 1877.
[4] G.X. Zhang, N.A. Yong-Lin, J.B. Guo, A new optical noncontact probe with four incidence lights and a receptor, Nanotechnol. Precis. Eng. (2006).
[5] K.Q. Lu, W. Wang, Z.C. Chen, Calibration of laser beam-direction for point laser sensors, Opt. Precis. Eng. 18 (2010) 880–886.
[6] U. Mutilba, E. Gomezacedo, G. Kortaberria, Traceability of on-machine tool measurement: a review, Sensors 17 (2017) 1605.
[7] C. Mentin, R. Priewald, E. Brenner, Accurate light source position estimation for a laser triangulation measurement device using particle swarm optimization, Measurement (2018).
[8] K.Q. Lu, W. Wang, Z.C. Chen, Calibration of laser beam-direction for point laser sensors, Opt. Precis. Eng. 18 (2010) 880–886.
[9] L.Y. Zhang, Y.I. Hong-Ming, S.L. Liu, Linear calibration for on-machine measurement of laser probe pose, Opt. Precis. Eng. 24 (2016) 681–689.
[10] B. Li, F. Li, H. Liu, A measurement strategy and an error-compensation model for the on-machine laser measurement of large-scale free-form surfaces, Meas. Sci. Technol. 25 (2014) 5204.
[11] B. Sun, A new error compensation strategy on laser displacement sensor in free-form surface measurement, Optifab (2015).
[12] B. Li, B. Sun, C. Lei, Application of laser displacement sensor to free-form surface measurement, Opt. Precis. Eng. 23 (2015) 1939–1947.
[13] S. Ibaraki, S. Goto, K. Tsuboi, Kinematic modeling and error sensitivity analysis for on-machine five-axis laser scanning measurement under machine geometric errors and workpiece setup errors, Int. J. Adv. Manuf. Technol. 2 (2018) 1–12.
[14] S. Ibaraki, N. Yu, Formulation of the influence of rotary axis geometric errors on five-axis on-machine optical scanning measurement—application to geometric error calibration by “chase-the-ball” test, Int. J. Adv. Manuf. Technol. 2 (2017) 1–11.
[15] Z. Dong, X. Sun, C. Chen, A fast and on-machine measuring system using the laser displacement sensor for the contour parameters of the drill pipe thread, Sensors 18 (2018) 1192.
[16] S. Li, X. Jia, M. Chen, Error analysis and correction for color in laser triangulation measurement, Optik 168 (2018).
[17] T. Mueller, E. Reithmeier, Image segmentation for laser triangulation based on Chan–Vese model, Measurement 63 (2015) 100–109.